

Study for TIG–MIG hybrid welding process

Shuhei Kanemaru · Tomoaki Sasaki · Toyoyuki Sato ·
Hisashi Mishima · Shinichi Tashiro · Manabu Tanaka

Received: 27 October 2012 / Accepted: 1 August 2013 / Published online: 22 August 2013
© International Institute of Welding 2013

Abstract Tungsten inert gas (TIG) and metal inert gas (MIG) welding are the most popular gas-shielded arc-welding processes used in many industrial fields. MIG welding is a high-efficiency process compared to TIG welding. However, improvements are needed to reduce spatter and improve weld metal toughness. Although pure argon shielding gas is desirable for weld metal toughness, MIG arcs are unstable in pure Ar to the extent that executing welding is difficult. We have found that MIG arcs become stable even using pure argon by simply using a hybrid TIG and MIG system. This process has the possibility of becoming a new welding process giving high quality and efficiency. In this study, we investigate the influence of the balance of current between the TIG and MIG arcs, which is most important in determining arc stability and arc penetration. We have confirmed the suitable range of conditions both experimentally and through numerical simulation and have applied this process for butt and fillet joints. We show that the welding time can be reduced to 17~44 % of the time required using a conventional TIG process.

Keyword A TIG welding · MIG welding · Argon · Shielding gases · Hybrid welding · Efficiency

1 Introduction

Tungsten inert gas (TIG) and metal inert gas (MIG) welding are the most popular gas shielded arc welding processes used

in many industrial fields. TIG welding is a high-quality process which has features of less spatters and better weld bead surfaces than welding using MIG with pure Ar. However, improvement in the efficiency of TIG welding is needed because of its slow speed and the small amount of deposited metal. On the other hand, MIG welding is a high-efficiency process with high rates of metal deposition, but still needs improvements in quality, spatter production, oxidation of the bead surface, and weld metal toughness [1].

For MIG welding, although pure argon shielding gas is desirable for weld metal toughness, the MIG arc is unstable in pure argon because of instabilities in the cathode spots on the base metal surface. As a result, there are problems such as weld defects and irregularity of the weld bead [2, 3]. If the shielding gas includes a small amount of an oxidizing gas such as oxygen or carbon dioxide, arc stability is improved and suitable welding execution is possible. Thus, mixed gases of Ar+O₂ or Ar+CO₂ are used for conventional MIG welding. However, these gases are used, it is impossible to avoid the oxidation of the bead surface and increased oxygen content in the weld metal, which causes a decrease of weld metal toughness.

We have found that MIG arcs become stable, even with pure argon, by adopting a simple hybrid system of TIG and MIG. With a TIG–MIG hybrid arc system, the cathode spots of MIG arcs do not behave unstably, and stable welding becomes possible [4]. Therefore, this process has the possibility as becoming a new type of welding process combining the high quality of TIG with the high efficiency of MIG.

Use of hybrid multi-heat sources is a useful method to solve problems which cannot be solved by using a single heat source. Various hybrid welding processes which have been used previously are now discussed [5–7]. The double-electrode GMAW and arcing-wire GTAW is a GMAW or GTAW system applied with a bypass current from an additional electrode. The aim is to increase the deposition rate without increasing heat input [8–15]. Although this system is similar to the present study, there are differences. For arc stability in pure inert gases, we use a simple adjustment of the basic current balance and also a suitable

Doc. IIW-2406, recommended for publication by Commission XII “Arc Welding Processes and Production Systems.”

S. Kanemaru (✉) · T. Sasaki · T. Sato
TAIYO NIPPON SANSO Corporation, Tokyo, Japan
e-mail: Syuhei.Kanemaru@tn-sanso.co.jp

H. Mishima · S. Tashiro · M. Tanaka
Joining and Welding Research Institute Osaka University, Osaka,
Japan

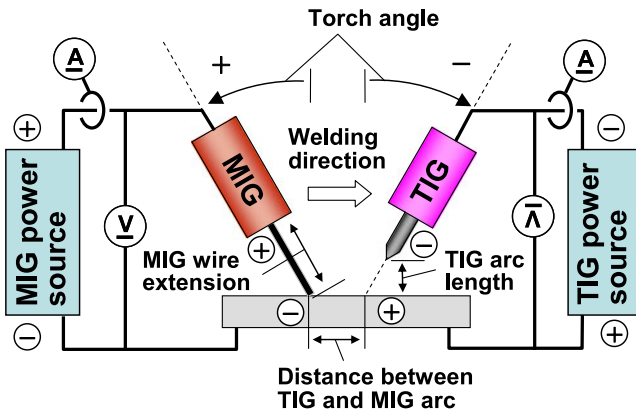


Fig. 1 Schematic diagram of experimental set up

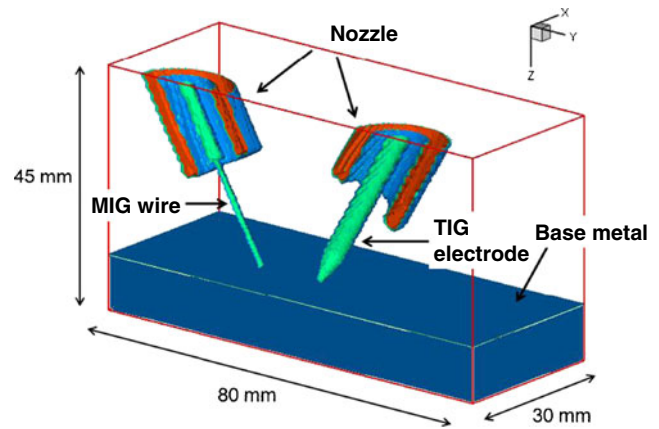


Fig. 2 Schematic diagram of simulation model

electrode configuration, without the need for special properties of the power source or special circuits of the apparatus.

In this study, we investigate the influence of the TIG–MIG current balance, which is the most important condition that affects arc stability and arc penetration. We confirm the suitable range of currents by experiments and numerical simulations. We applied this process to butt joints, and show that the welding time can be reduced to about 17–44 % of the time for conventional TIG welding.

2 Experimental procedures and numerical simulation models

Figure 1 shows the dimensions and configuration of the experimental welding torches and power sources. Table 1 shows the welding conditions of this study. In the configuration, the TIG arc was leading and the MIG arc trailing, with a

specified distance between the two. The TIG arc was ignited first, a weld pool was formed on the surface of the base metal, and then the MIG arc was ignited.

The first experiment was performed to determine the stability of the TIG–MIG system for the conditions shown in Table 1. Comparisons were made of arc stability, bead appearance, cross section, and current–voltage characteristic, with results for conventional TIG and MIG arcs. The shielding gas was pure Ar and Ar+2 % O₂, which are popular MIG shielding gases.

The second experiment was performed to evaluate the influence of the current balance between TIG and MIG. MIG current was fixed to 270 A, the metal transfer mode was set up as streaming transfer, and the TIG current was in the range of 150–500 A.

To compare with the above two experiments, we did a numerical simulation based on the current path and temperature distribution of the TIG–MIG hybrid arc. To simulate the

Table 1 Welding conditions

Parameters	1st experiment (Basic condition)	2nd experiment (Change of TIG current)	3rd Experiment (Application for joints)
Joint	Bead on plate		Butt joint, fillet weld
Base metal	Stainless steel type304, t12mm		Stainless steel type304, t12mm and t6mm
Current	TIG : 350A MIG: 270 A	TIG: 150~500 A MIG: 270 A	TIG: 400A MIG: 280 A
Welding speed	30 cm/min		
Wire feed speed	10 m/min		11 m/min
Distance between TIG and MIG arc	4 mm		
TIG electrode	DCEN, La ₂ O ₃ , Ø 4.0 mm, Tip angle: 30°		
TIG arc length	5 mm		
MIG wire	DCEP, type308, Ø 1.2 mm		
MIG wire extension	25 mm		
Torch angle TIG/MIG	TIG–MIG:–30/+30 MIG: +15	–30/+30	
Shielding gas	Ar		Ar, Ar+He

asymmetric interaction of the TIG and MIG arcs, a three-dimensional model was used as shown in Fig. 2. Main assumptions on the model were as follows:

- (1) LTE approximation holds for the arc plasma.
- (2) All flows are laminar flow.
- (3) Electrodes are a solid phase.

- (4) The surface of the weld pool is flat and does not change shape.
- (5) Metal transfer of MIG wire is only considered for heat transport.

The detail of equations and assumptions is reported in our previous report [16].

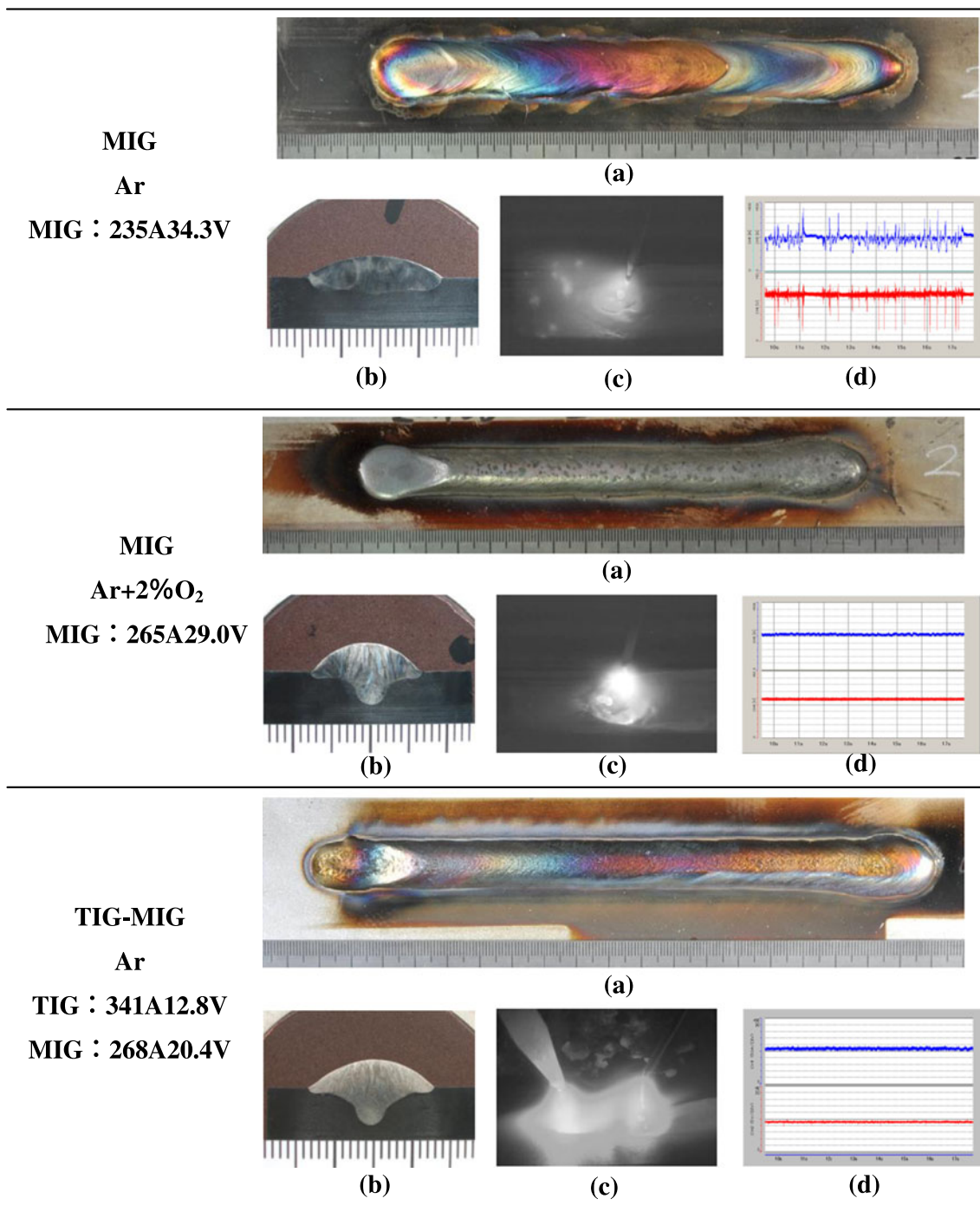


Fig. 3 Experimental data of TIG–MIG hybrid welding on basic condition **a** bead appearance, **b** cross section, **c** image of high-speed camera, and **d** current–voltage wave of MIG

In the final experiment, test plates were welded with butt joints and a fillet joint. The purpose of this experiment was to evaluate the weldability of practical joints and to compare efficiency and quality with conventional TIG and MIG welding processes. Efficiency was assessed by comparing welding times with times of standard TIG conditions. We made V-notched sharp impact tests and also measurements of oxygen content in the weld metal to evaluate weld bead quality.

3 Results and discussion

3.1 Stability of the TIG–MIG hybrid system

3.1.1 Experimental results

Figure 3 compares bead appearance, cross sections, images from a high-speed camera, and current–voltage characteristics of conventional MIG welding with results from the TIG–MIG hybrid system.

The bead appearance of conventional MIG using pure argon showed irregularity of the bead and a clean width with no oxidation around the bead, which is evidence of irregular behavior of the cathode spots. On the other hand, MIG and the TIG–MIG hybrid with Ar+O₂ shield gas had no irregularities of weld bead or a clean width. It is suggested that the MIG arc was stable because of the effect of the oxygen content in the shielding gas. Furthermore, the bead surface of the TIG–MIG hybrid was not oxidized by the Ar+O₂ shielding gas. Comparisons of penetration depth could not be made because large heat inputs were not possible for use with pure argon because of the instability of these arcs.

Observations of the TIG–MIG hybrid arcs indicated repulsion effects on both arcs by electromagnetic forces from the mutual arc currents. The metal transfer mode was stable streaming transfer without spatter. Curves of current and voltage indicated stable welding without any short circuit from wire to base metal. On the other hand, for MIG with pure argon shielding, arc instabilities were indicated both from high-speed camera photographs and current–voltage curves.

3.1.2 Comparison with results of numerical simulations

Figure 4 shows the results of numerical calculations of the temperature distribution of the TIG–MIG hybrid arc. The repulsion of both arcs is shown in the simulation results, and is the same as indicated by the experimental data. Thus, the form of the arc from the numerical temperature distributions is roughly in agreement with experimental observations.

Figure 5 shows the current density distribution of the TIG–MIG hybrid arc. Current values are classified into five paths as illustrated in Fig. 5 as follows:

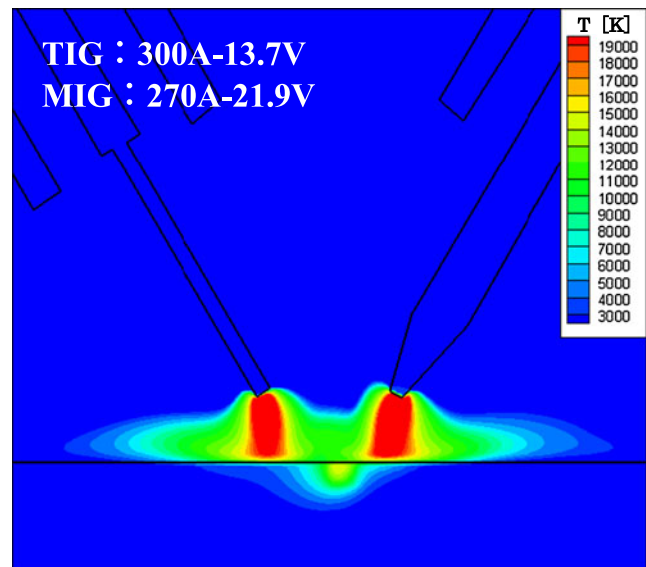


Fig. 4 Temperature distribution of each model

- (1) TIG electrode
- (2) TIG electrode–base metal
- (3) TIG electrode–MIG wire
- (4) MIG wire–base metal
- (5) MIG wire

Figure 6 shows high-speed camera pictures of the TIG–MIG hybrid arc and the TIG arc under the same conditions as the simulations. The current–voltage curves of the TIG–MIG hybrid and conventional TIG for both simulations and experimental results are shown in the each figure. The TIG voltage for conventional TIG is higher than the TIG–MIG hybrid, although

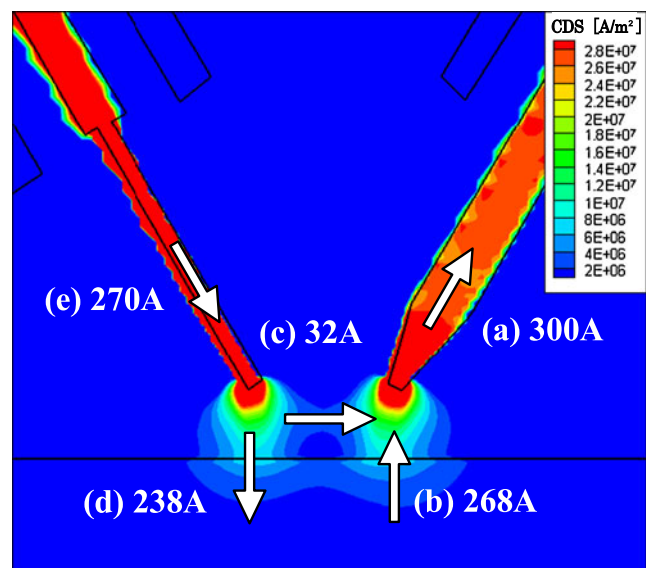
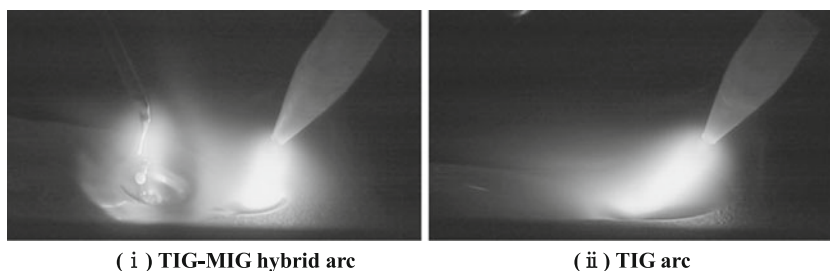


Fig. 5 Simulation results current density distribution and current path classification

Fig. 6 Image of high-speed camera picture and current–voltage value



both current values are the same, which suggests the generation of a direct current path between the TIG and MIG electrodes in the experiment. The results support the validity of the numerical model.

3.2 Influence of the balance of current between TIG and MIG

3.2.1 Experimental results

Figure 7 shows the bead appearance and the cross section as a function of TIG current in the range of 150~500 A. MIG current was fixed at 270 A and the wire feed rate fixed at 10m/min, to maintain metal transfer in the streaming mode. A stable arc was generated in the range of TIG current from

250 to 500 A, i.e., in the range such that TIG current is greater than MIG current. A clean area was not seen around the bead in this current range. On the other hand, with the TIG current range from 150 to 200 A, TIG current is less than MIG current, and the MIG arc was unstable, producing much spatter. Also, a clean area was seen around the bead, as in the case of pure argon-shielded MIG welding.

The penetration depth increased for TIG current in the range of TIG current greater than MIG current. However, in the range of TIG current less than MIG current, the penetration depth was independent of TIG current. These results suggest that the TIG current needs to be greater than the MIG current for arc stability. Then, increased TIG current increases the penetration depth.

500A [17V/19V]			
400A [14V/23V]			
300A [13V/23V]			
200A [1.4V/34V]			
0A [-/38V]			
TIG Current [TIG/MIG voltage]	Bead appearance	Cross section	Image of high speed camera

Fig. 7 Influence of leading TIG current on experimental results

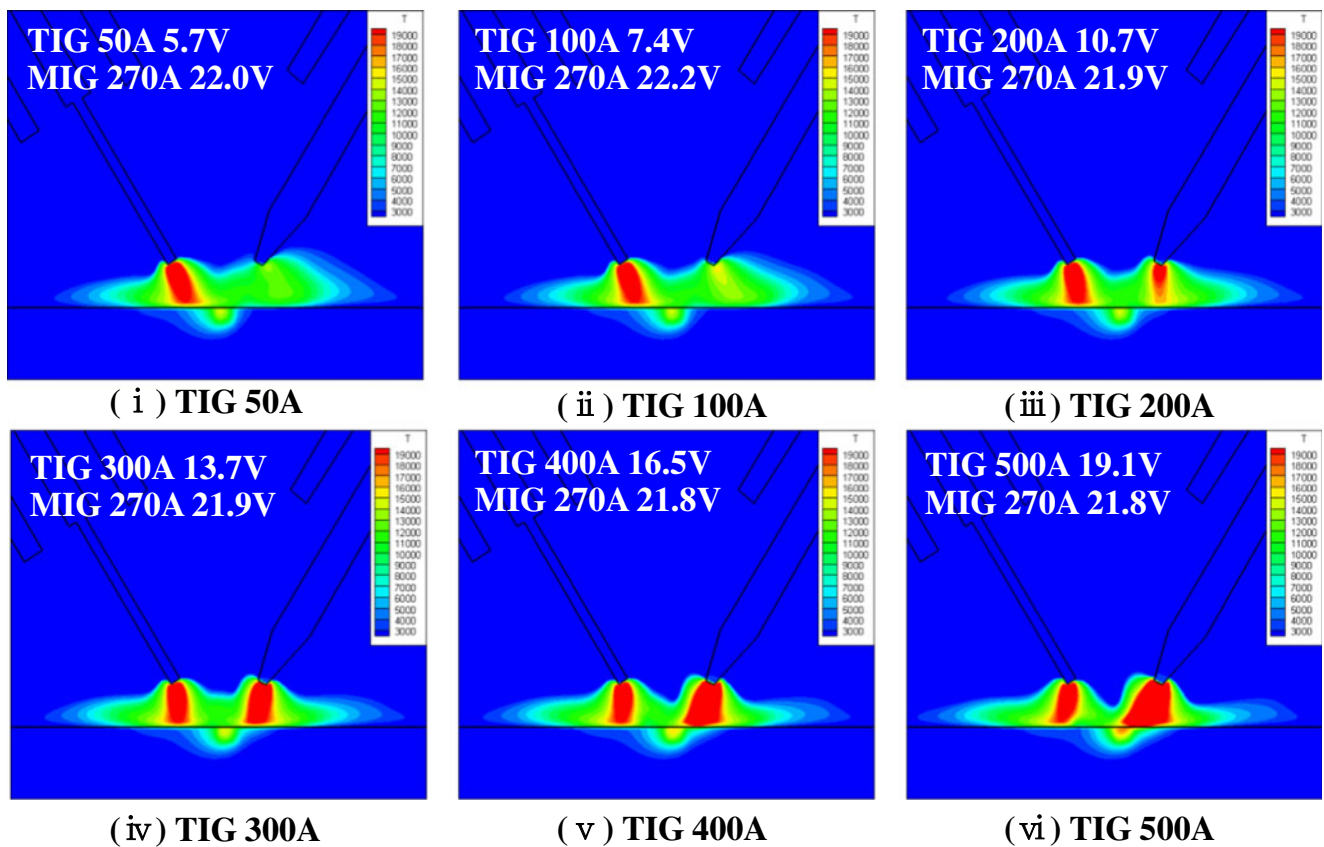


Fig. 8 Temperature distribution of each condition of TIG current 50~500 A

3.2.2 Comparison with results of numerical simulation

Figure 8 shows temperature distribution from the numerical simulation, and Table 2 shows the current values of each path under the condition of TIG current 50~500 A. The following results were obtained:

- (1) The direct current path (c) had a maximum of 32 A for a TIG current of 300 A.
- (2) The value of the current path (b) increased along with TIG current because of saturation of the current in the path (c).
- (3) Because electromagnetic forces depend on the current, increase of the value of current in path (b) causes increased repulsion. Thus, the repulsion between both arcs increased, with TIG current and, as a result, MIG arc is in opposite direction in condition (v) and (vi).

Table 2 Value of classified current pass on each condition of value (a)

Input	(a) TIG electrode	50	100	200	300	400	500
Output	(b) TIG electrode–base metal	30	67	172	268	372	480
	(c) TIG electrode–MIG wire	20	23	28	32	28	20
	(d) MIG wire–base metal	250	247	242	238	242	250
Input	(e) MIG wire	270					

- (4) As a result of separation of both arcs by increases in repulsion, the value of current in path (c) decreases in condition (v) and (vi).

Figure 9 shows the comparison of simulation results with experimental results, for the correlation of two property as shown below:

- The share of value of current paths (b) to current path (a)
- The change of the experimental penetration depth from an increase of TIG current

The share of current (b) compared with (a) depends on TIG current and becomes more than 80 % in the range of the TIG

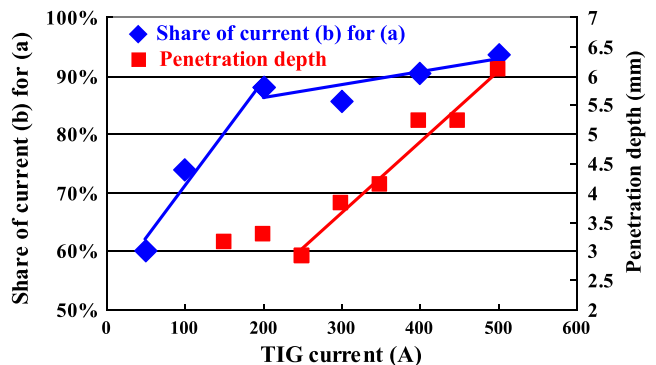


Fig. 9 Comparison simulation results and experimental results

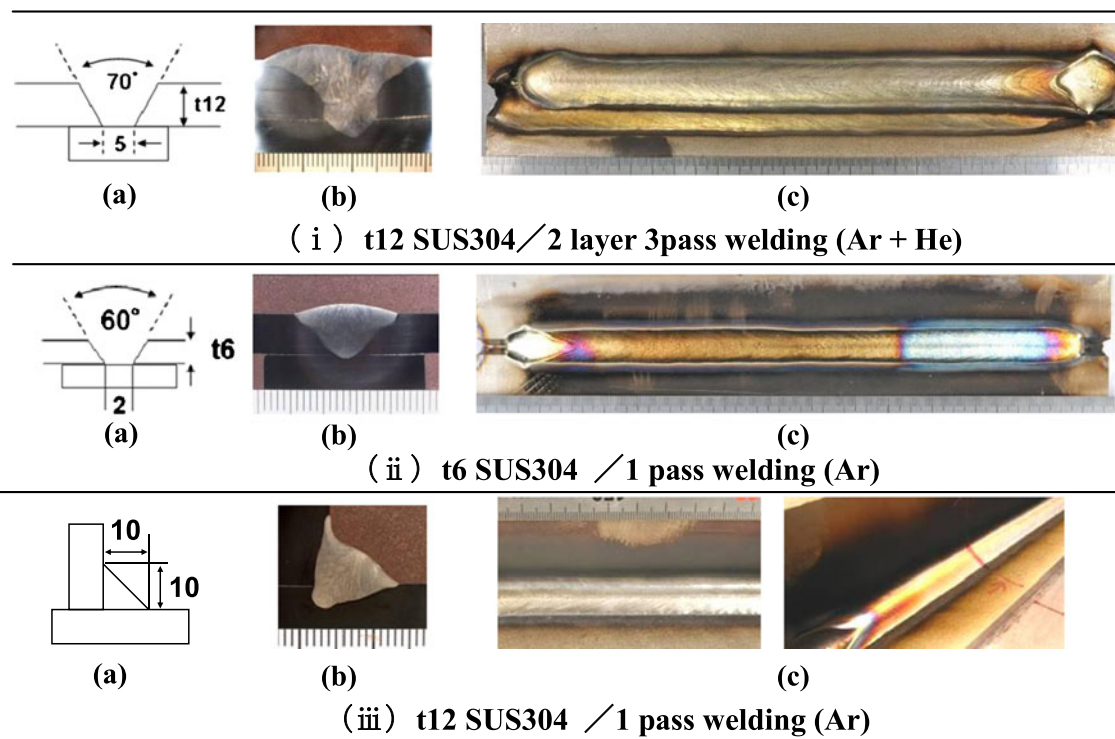


Fig. 10 Experimental data of application for practical joints **a** form of groove, **b** cross section, and **c** bead appearance

current from 200 to 500 A. For low currents in the range from 50 to 200 A, it is thought that the TIG current is insufficient for melting the base metal. Then most of the current becomes the direct current of path (c), which does not contribute to the heat input of the base metal. Thus, the development of current in path (b), which contributes to heat input, becomes effective for TIG currents of more than 200 A.

3.3 Application for the practical joints

Figure 10 shows results for the welding of butt joints and fillet joints using the TIG–MIG hybrid system. For each weld thickness, good joints were made without detection of defects using radiography. There was no appearance of surface oxidation of

the bead, as occurred for conventional TIG welding using pure inert shielding gas.

Table 3 shows the results of efficiency based on welding time, comparing the hybrid system with standard TIG welding. Only welding speed and the number of passes were considered for efficiency. The welding time was reduced to about 17~44 % of the times for conventional TIG, confirming a significant improvement in efficiency using the hybrid system.

Table 4 and Table 5 shows the results of V-notch sharp impact tests and measurements of the oxygen content in the weld metal, base metal, and MIG wire. Because of low oxygen contained in the weld metal and base metal, a significant high absorbed energy value of about 200 J was obtained. Thus, high-weld metal toughness, equivalent to standard TIG welding, is expected.

Therefore, these results suggest that the welding time can be reduced to about 17~44 % of the conventional TIG welding process without any degradation in quality by using the TIG–MIG welding process.

Table 3 Comparison of welding time for TIG and TIG–MIG

Parameter	Welding process	(a) t12 butt joint	(b) t6 butt joint	(c) t13 fillet joint
Welding speed (cm/min)	TIG	5~20	10~15	5~10
	TIG–MIG	30	30	30
Number of pass	TIG	6	2	2
	TIG–MIG	4	1	1
Welding time (min/m) (ratio of time)	TIG	30	13.3	20
	TIG–MIG	13.3 (44 %)	3.3 (25 %)	3.3 (17 %)

Table 4 Result of V-notched sharp impact test (condition (a))

Test specimen NO.	Absorbed energy (J)	
	Single	Ave
1	197	
2	190	195
3	199	

Table 5 Oxygen content of weld metal (condition (a))

Sample	O (ppm)
Weld metal	25
Base metal	46
Wire	34

4 Conclusion

In this study, we found that a pure argon-shielded MIG arc can become stable by using a simple TIG and MIG hybrid system. The influence of TIG current on the welding properties such as stability of the arc, penetration depth, and repulsion between both arcs were investigated by experiments and numerical simulations. Tests for efficiency and weld quality have been made for practical joints and compared with results from conventional TIG and MIG welding. The following conclusions have been made:

- (1) In the TIG–MIG hybrid systems, both arcs perform well. MIG arcs are stable, without spatter or irregular behavior of cathode spots, even though the shielding gas is pure Ar.
- (2) For the TIG–MIG hybrid arc, it is suggested from both experimental and numerical simulation results that a current path is generated between TIG and MIG electrodes. It is thought that this phenomena contributes to the stability of the MIG arc using pure argon gas.
- (3) For the current balance, the TIG and MIG arcs of the hybrid system, the TIG current needs to be larger than the MIG current to keep the MIG arc stable when using pure argon. Penetration depth increases with increase of TIG current as long as the TIG current is larger than the MIG current.
- (4) Good butt and fillet joints were obtained with no defects detected by radiography. The welding time is reduced to about 17~44 % of the times used by conventional TIG. Moreover, it is confirmed from V-notch sharp impact tests and the measurement of oxygen content in the weld metal that toughness should be equivalent to standard TIG welding.

References

1. Kamiya H, Fujita T, Enjo Y (1985) Kikkuchi: oxygen content and fracture toughness on MIG weld metal of SUS 304 steel. *Quart J Japan Weld Soc* 3(3):138–145 (in Japanese)
2. Matsuda F, Ushio M, Saikawa S, Maruyama Y, Araya T (1983) Study on GMA welding for 9 % Ni steel with similarly composed nickel alloy wire. *Journal of Japan Welding Society* 82(3):66–73, in Japanese
3. Zenitani S, Nakamura T, Hiraoka K, Shinozaki K (2007) Ar–MIG arc behavior in local addition of small amount of oxygen into shielding gas. *Quart J Japan Weld Soc* 25(1):187–195 (in Japanese)
4. Kanemaru S, Sasaki T, Sato T, Tanaka M (2012) Basic study of TIG–MIG hybrid welding process. *Quart J Japan Weld Soc* 30(1):29–34 (in Japanese)
5. Qin GL, Lei Z, Lin SY (2007) Effect of Nd:YAG laser+pulsed MAG arc hybrid welding parameters on its weld shape. *Sci Technol Weld Joi* 12(1):79–86
6. Ueyama T, Ohnawa T, Tanaka M, Nakata K (2005) Effects of torch configuration and welding current on weld bead formation in high-speed tandem pulsed gas metal arc welding of steel sheets. *Science and Technology of Welding & Joining* 10(6):750–759
7. Kobayashi K, Matusoka T, Ushio M, Tanaka M (2003) The elucidation of twin-electrodes TIG arc phenomenon. *Preprints of The National Meeting of Japan Welding Society* 73:194–195 (in Japanese)
8. Li KH, Zhang YM (2007) Metal transfer in double-electrode gas metal arc welding. *J Manuf Sci E-T ASME* 129(6):991–999
9. Li KH, Chen JS, Zhang YM (2007) Double-electrode GMAW process and control. *Weld J* 86(8):231s–237s
10. Li KH, Zhang YM (2008) Consumable double-electrode GMAW part I: the process. *Weld J* 87(1):11s–17s
11. Li KH, Zhang YM (2008) Consumable double-electrode GMAW part II: monitoring, modeling, and control. *Weld J* 87(2):44s–50s
12. Li KH, Zhang YM, XU P, Yang FQ (2008) High-strength steel welding with consumable double-electrode gas metal arc welding. *Weld J* 87(3):57s–64s
13. Shi Y, Liu X, Zhang Y, Johnson M (2008) Analysis of metal transfer and correlated influences in dual-bypass GMAW of aluminum. *Weld J* 87(9):229s–236s
14. Li K, Wu C (2009) Mechanism of metal transfer in DE-GMAW. *J Mater Sci Technol* 25(3):415–418
15. Chen JS, Lu Y, Li XR, Zhang YM (2012) Gas tungsten arc welding using an arcing wire. *Weld J* 91(5):216s–269s
16. Kanemaru S, Sasaki T, Sato T, Mishima H, Tashiro S, Tanaka M (2012) Study for the arc phenomena of TIG–MIG hybrid welding process by 3D numerical analysis model. *Quart J Japan Weld Soc* 30(4):323–330 (in Japanese)